

Analysis and applications of 3D rectangular metallic waveguides

Mohamed A. Swillam, and Amr S. Helmy

Department of Electrical and Computer Engineering, University of Toronto, Toronto, M5S 3G4, Canada.
m.swillam@utoronto.ca

Abstract: Plasmonic modes in rectangular metallic waveguides are analyzed in depth and are demonstrated to possess attractive properties for different applications. Their dispersion characteristics allow for wide range of applications including slow and fast light, metamaterial, low loss energy transmission, and opportunities for sensing devices. The sensitivity of this waveguide configuration is higher than its counterparts and can reach four times the sensitivity of the MIM structures. The characteristics of the TM_{10} mode are demonstrated. Its applications for sensing, low propagation loss with relaxed practical dimension are also highlighted. A high effective index of more than 30 is also obtainable for the TE_{01} mode for slow light operation. A non resonant negative index material with isotropic polarization in the visible region is also proposed using this waveguide structure.

©2010 Optical Society of America

OCIS codes: (240.6680) Surface plasmons; (250.5403) Plasmonics; (160.3918) Metamaterials; (130.2790) Guided waves; (280.4788) Optical sensing and sensors

References and links

1. S. A. Maier, *Plasmonics: Fundamentals and Applications*, (Springer, 2007).
2. G. Veronis, and S. Fan, "Modes of Subwavelength Plasmonic Slot Waveguides," *J. Lightwave Technol.* **25**(9), 2511–2521 (2007).
3. W. L. Barnes, A. Dereux, and T. W. Ebbesen, "Surface plasmon subwavelength optics," *Nature* **424**(6950), 824–830 (2003).
4. J. Homola, S. S. Yee, and G. Gauglitz, "Surface plasmon resonance sensors: review," *Sens. Actuators B Chem.* **54**(1-2), 3–15 (1999).
5. R. D. Harris, and J. S. Wilkinson, "Waveguide surface plasmon resonance sensors," *Sens. Actuators B Chem.* **29**(1-3), 261–267 (1995).
6. J. Homola, "Present and future of surface plasmon resonance biosensors," *Anal. Bioanal. Chem.* **377**(3), 528–539 (2003).
7. J. A. Dionne, L. A. Sweatlock, H. A. Atwater, and A. Polman, "Plasmon slot waveguides: Towards chip-scale propagation with subwavelength-scale localization," *Phys. Rev. B* **73**(3), 035407 (2006).
8. H. J. Lezec, J. A. Dionne, and H. A. Atwater, "Negative refraction at visible frequencies," *Science* **316**(5823), 430–432 (2007).
9. T. Yang, and K. B. Crozier, "Analysis of surface plasmon waves in metaldielectric- metal structures and the criterion for negative refractive index," *Opt. Express* **17**(2), 1136–1143 (2009).
10. J. A. Dionne, E. Verhagen, A. Polman, and H. A. Atwater, "Are negative index materials achievable with surface plasmon waveguides? A case study of three plasmonic geometries," *Opt. Express* **16**(23), 19001–19017 (2008).
11. A. Alù, N. Engheta, A. Alu', "Optical nanotransmission lines: synthesis of planar left-handed metamaterials in the infrared and visible regimes," *J. Opt. Soc. Am. B* **23**(3), 571–583 (2006).
12. A. Alù, N. Engheta; A. Alu', "Light squeezing through arbitrarily shaped plasmonic channels and sharp bends," *Phys. Rev. B* **78**(3), 035440 (2008).
13. F. J. García-Vidal, L. Martín-Moreno, E. Moreno, L. Kumar, and R. Gordon, "Transmission of light through single rectangular hole in a real metal," *Phys. Rev. B* **74**(15), 153411 (2006).
14. T. W. Ebbesen, H. J. Lezec, H. F. Ghaemi, T. Thio, and P. A. Wolff, "Extraordinary optical transmission through sub-wavelength hole arrays," *Nature* **391**(6668), 667–669 (1998).
15. E. Feigenbaum, and M. Orenstein, "Modeling of Complementary (Void) Plasmon Waveguiding," *J. Lightwave Technol.* **25**(9), 2547–2562 (2007).
16. R. Gordon, and A. Brolo, "Increased cut-off wavelength for a subwavelength hole in a real metal," *Opt. Express* **13**(6), 1933–1938 (2005).
17. M. A. Swillam, M. H. Bakr, and X. Li, "Efficient Design of Integrated Wideband Polarization Splitter/Combiner," *J. Lightwave Technol.* **28**(8), 1176–1183 (2010).
18. *Electromagnetics Module User's Guide* (Comsol, 2007), Sweden. <http://www.comsol.com>.

19. E. D. Palik, *Handbook of optical constants of solids*, (Academic Press, Inc. 1985).
 20. *FDTD Solutions Reference Guide*, (Lumerical Solutions, 2009).
 21. A. Karalis, E. Lidorikis, M. Ibanescu, J. D. Joannopoulos, and M. Soljacić, "Surface-plasmon-assisted guiding of broadband slow and subwavelength light in air," *Phys. Rev. Lett.* **95**(6), 063901 (2005).
 22. V. G. Veselago, "The electrodynamics of substances with simultaneously negative values of ϵ and μ ," *Sov. Phys. Usp.* **10**(4), 509–514 (1968).
 23. H. Shin, and S. Fan, "All-angle negative refraction for surface plasmon waves using a metal-dielectric-metal structure," *Phys. Rev. Lett.* **96**(7), 073907 (2006).
 24. E. Feigenbaum, N. Kaminski, and M. Orenstein, "Negative dispersion: a backward wave or fast light? Nanoplasmonic examples," *Opt. Express* **17**(21), 18934–18939 (2009).
 25. R. W. Boyd, and D. J. Gauthier, "'Slow' and 'Fast' Light," *Prog. Opt.* **43**, 497–530 (2002).
-

1. Introduction

Surface plasmon polariton (SPPs) waveguides have attracted enormous attention in the last decade due to their useful ability to guide the light on the nanometer scale with remarkably useful characteristics. Unlike conventional photonic waveguides, which are based on total internal reflection (TIR), rectangular 3D metallic waveguides can guide light utilizing SPP-like modes with no restriction on the optical properties of the core region. This is mainly due to the significant mismatch at the interface between dielectrics and metals at optical frequencies [1–3]. This property has significant impact on sensing application as it allows for maximum overlap between the optical field and the material under test [4–8]. In addition, the tightly confined optical field obtained using SPP waveguides provides a solution for the size incompatibility of electronic components and conventional photonic devices. This allows for the utilization of optical interconnects in electronic integrated circuits to circumvent the limitations posed by electronic interconnects.

Using SPP waveguides as a building block for optical devices enables not only sensing and optical interconnects but also extends to unconventional electromagnetics phenomena such as extra ordinary transmission (EOT) and negative index optical materials. These effects have been exploited in wide range of interesting applications. Including sub-wavelength focusing and phase and group delay effects. Among the different SPP waveguide structures the Metal-Insulator-Metal (MIM) and Insulator-Metal-Insulator (IMI) attract the most attention due to their relative simplicity for fabrication. MIM configuration has been also used as a slot waveguide structure to guide the light in low index region mainly for sensing and interconnects applications [7]. Negative index of refraction and slow light applications have been also proposed theoretically and demonstrated experimentally for these structures [8–11].

Despite of the several demonstrations of useful functions in MIM waveguides, these functions are only available for a single polarization. In order to obtain them for both polarizations, rectangular metallic waveguide design may be used. The rectangular metallic waveguide has fundamentally different characteristics than MIM and IMI based waveguides. These characteristics include for example the cutoff wavelength, and the properties for various polarization types. Many interesting phenomena occur if the rectangular waveguide is operating close to its cutoff wavelength. These phenomena include high transmission and energy tunneling [12]. The near cutoff operation of this waveguide has been also proven to be the main cause of extra ordinary transmission from single rectangular hole [13], or arrays of holes [14]. Despite its attractive applications and unique properties, most of the studies for this waveguide type have been limited to a certain effect or phenomenon at specific wavelength band.

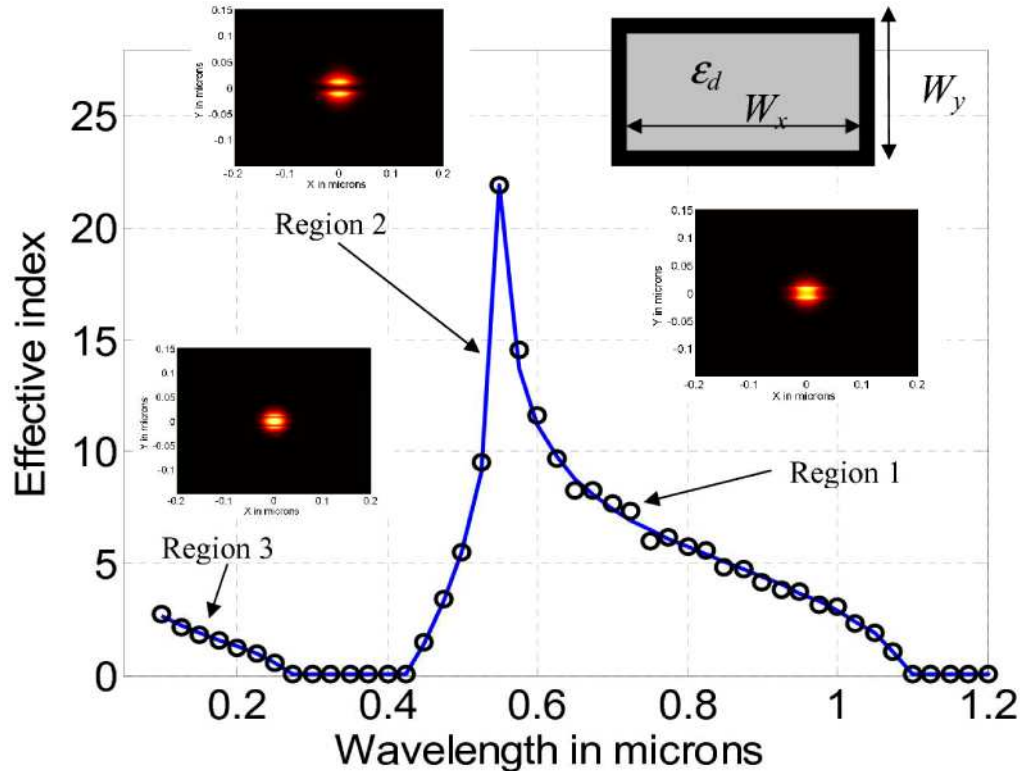


Fig. 1. The dispersion characteristics of the fundamental y-polarized mode of rectangular waveguide 20x40 nm with silver metal walls and filed dielectric of refractive index 3.5 using finite difference frequency domain solver (-) and using Comsol (o).

In this work, we analyze the metallic rectangular waveguide, while investigating its operating characteristics over the various different operating regimes. The similarities and differences between this waveguide and the MIM structures are also highlighted. The characteristics of the fundamental TM_{10} mode, which only exists in this waveguiding structure in contrast to MIM structures, are also discussed. Different applications of current interest can take place in its different operating regimes. Those are also illustrated and discussed in details. For example, novel designs for energy tunneling and low loss transmission at much larger dimensions than those reported in [12] using TM_{10} are reported. The high sensitivity of the rectangular waveguide for the core material is also demonstrated for sensing applications. This waveguide has much higher sensitivity than MIM structures over the entire operating band. We demonstrate that the sensitivity can be four times higher than the MIM sensitivity at wavelengths close to cutoff. Working close to the cutoff also allows for very low propagation losses due to the small value of the effective index [12,15,16].

We start by briefly describing the key guided modes in Section 2. The application of the rectangular waveguide in sensing and energy transmission is discussed in Section 3. In this section, near cutoff, low loss waveguide design is proposed based on TM_{10} , which allows for more relaxed physical dimensions and longer interaction lengths with the sensing material. In Section 4, the capability of the rectangular waveguide to guide modes with very high effective index is also demonstrated. A high effective index of more than 30 can be obtained using this structure. This effect can be exploited to produce ultra compact integrated optical delays for on chip interconnect applications. Polarization insensitive slow and fast light and negative refraction are also discussed in this section. Finally, the conclusion is given in Section 5.

2. Modal analysis of guided modes

In this section, the various key guided modes supported by the rectangular waveguide are studied and the conditions at which these modes may exist are elucidated. For this purpose, the dispersion characteristics are calculated using finite difference frequency domain mode solver with perfect matched layer (PML) employed as a boundary condition similar to the one utilized in [17]. All the results are also verified using a commercially available finite element technique, Comsol Multiphysics [18]. The material parameters of the metals are taken from [19]. The dispersion characteristics of the fundamental y -polarized mode of a rectangular waveguide filled with a dielectric material is calculated using both techniques and shown in Fig. 1. As shown in this figure, this dispersion curve has different characteristics in different regimes of operation. In Region 1, the field profile of the fundamental mode is similar to that of the TE_{01} mode of the metallic waveguide at microwave frequencies as shown in the inset of Fig. 1. Its behavior is distinct from that of the conventional MIM plasmon mode within this wavelength band; this rectangular waveguide mode has cutoff wavelength, which is not the case for similar modes of MIM structures. The cutoff wavelength of the fundamental TE_{01} has been recently studied and showed to be red shifted for real metals than the value obtained from microwave theory for perfect metals, which estimates the cutoff wavelength of the fundamental as $2W_x n_d$, where W_x is the width of the waveguide [16]. For Region 2, the waveguide exhibits negative group velocity or negative dispersion. The fundamental mode in this region is mainly a surface asymmetric mode as shown in the inset of Fig. 1. In this region, the waveguide can be exploited in several different applications such as fast light and as a building block negative refractive index media. The details of the characteristics of this region are discussed in Section 4. The fundamental mode in Region 3 is a conventional mode similar to those in dielectric optical waveguides and is based on TIR as shown in Fig. 1.

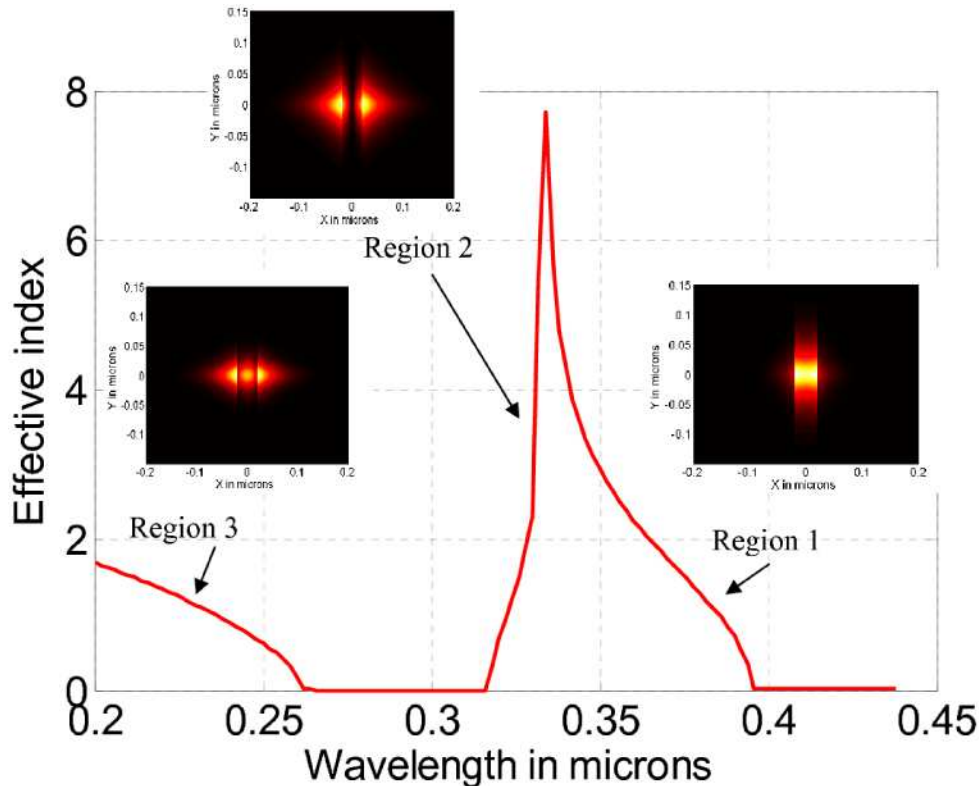


Fig. 2. The dispersion characteristics of the fundamental x -polarized mode of rectangular waveguide 20×40 nm with silver metal walls and filled dielectric of refractive index 3.5.

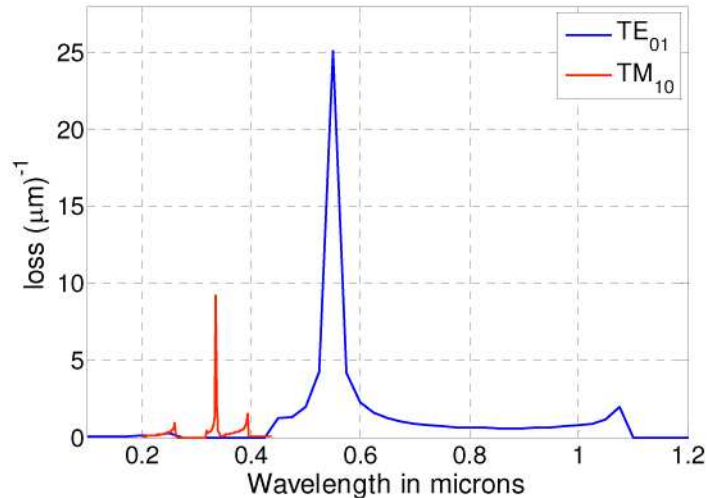


Fig. 3. The propagation loss of the fundamental x -polarized and y -polarized mode of rectangular waveguide 20×40 nm with silver metal walls and filed dielectric of refractive index 3.5.

Similar behaviour is obtained for the x -polarized electric field, i.e. the major field component is oriented in the same direction of the longer dimension of the waveguide W_x . The unique feature about this polarization is the fundamental mode in Region 1. In contrast to the y -polarized case, the fundamental mode profile in this region does not have a counterpart in the microwave regime as shown in the inset of Fig. 2. This mode is called TM_{10} as it does not correspond to any microwave mode of metallic waveguide. In addition, it is mainly transverse magnetic mode with one major field component. The cutoff wavelength of this mode is blue shifted in comparison to the TE_{01} case as shown in Fig. 2. This is mainly because it is controlled by the shorter dimension of the waveguide W_y . This blue shift can be a useful characteristic for some applications. For example, in order to obtain the same cutoff wavelength of the TE_{01} and the TM_{10} , the dimension of the later is much bigger than the former. Thus, for near cutoff applications, for example, the TM_{10} is a more useful mode to use as it relaxes the dimensions, while maintaining the same effect. The fundamental mode in Region 2 is also the asymmetric surface mode similar to the one in the TE case discussed earlier. The propagation loss of the TE_{01} and the TM_{10} is also calculated and shown in Fig. 3. It is clear from this figure that the losses increase only in the range at which the effective index is around its maximum value. However, the losses are decreasing close to the cutoff region.

Conventional optical modes based on TIR also exist for both polarizations, particularly in Region 1. However, these modes depend on the waveguide dimensions and always appear as higher order modes. Thus, their propagation constants are smaller than the plasmon mode in this region.

Within the rest of this work, the fundamental mode in each region is considered and its characteristics are carefully studied to explore its utilization in various applications. As can be inferred from the dispersion characteristics, the rectangular waveguide has significantly different properties in the different regions of operations. Different applications can utilize different regions. For example in Region 1, the modal and transmission characteristics of this waveguide are highly sensitive to the core material especially for operation close to the cutoff wavelength. Thus, at this wavelength, applications such as sensing and energy tunneling can be exploited. The regime at the border between Regions 1 and 2 has an effective index that can reach high values. Thus, it may be exploited in slow light applications. Conversely Region 2 in general can be exploited for fast light and negative index of refraction

applications. The sections of the paper that follow are devoted to further examine the performance attributes of these waveguides for the aforementioned applications.

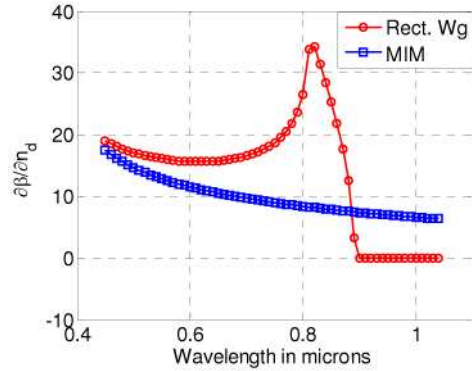


Fig. 4. The sensitivity of the propagation constant with respect to the refractive index of the filled material for both MIM and rectangular waveguide 360x600 nm TM_{10}

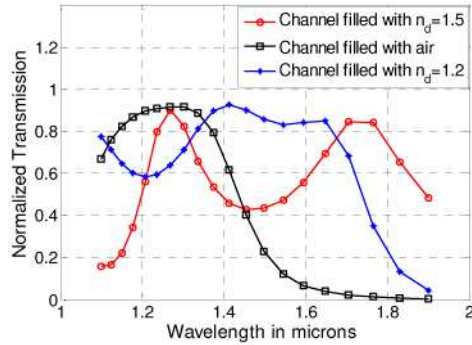


Fig. 5. The transmission characteristics through rectangular channel waveguide of length 1 microns in using the TM_{10} mode.

3. Rectangular waveguide in sensing and energy transmission applications

For this application, the waveguide is engineered to operate close to the cutoff wavelength. This effect is however not attainable using MIM configurations. Near the cutoff, the waveguide has very interesting capability of transporting the electromagnetic energy with minimum losses. This enhanced transmission is considered the main reason for extra ordinary transmission through hole arrays. This (EOT) is proved to occur at wavelength close to the cutoff wavelength of the fundamental mode of this hole [13]. The same effect has been also studied for energy transmission through rectangular waveguides working close to its cutoff. Within this wavelength regime the waveguide operates as an effective medium with epsilon near zero (ENZ) [12].

Most of the proposed applications for ENZ have exploited the TE_{01} mode for the waveguide using y-polarized light. The main drawback of this mode is the stringent requirement of small nanometer-scale waveguide dimensions to obtain the ENZ effect and hence obtain EOT characteristics. Such dimensions limit the practical use of these properties. In this work, we point out that the same effect can be obtained using the TM_{10} mode. The cutoff wavelength of this mode can be designed to take place for much larger dimensions than those for the TE_{01} . For example, the cutoff wavelength of 810 nm is obtained for the TE_{01} for dimensions of 20×200 nm, while for the TM_{10} the same cutoff wavelength can be obtained at 360×600 nm. Thus, this mode can be more suitable for energy transmission through sharp bends as well as for sensing application, where more practical dimensions are attainable.

In general, the rectangular waveguide is more sensitive to the core material filling than the MIM or slot waveguides. In addition, from a more practical point of view it provides 2D confinement for the core material, which can include liquids. It can also be designed as square waveguide with polarization insensitivity to the host material, which may be an enabling feature for several practical devices. Moreover, the rectangular waveguide becomes highly sensitive to the optical properties of the core material if it operates in the ENZ regime, i.e. close to its cutoff wavelength. The sensitivity of the rectangular waveguide is calculated with respect to the refractive index of the core material n_d and is shown in Fig. 4. The results are also compared with a MIM structure with the same dimension and similar field polarization. It is clear that the sensitivity of the rectangular waveguide is higher over the entire wavelength band. It also reaches four times the MIM sensitivity close to the cutoff wavelength of the waveguide. Both the TE_{01} and TM_{10} exhibit the same behavior for single mode operation.

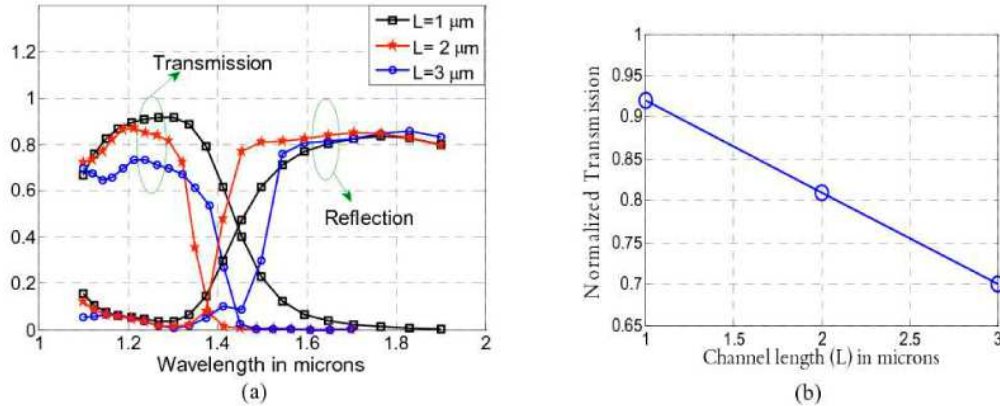


Fig. 6. The transmission characteristics through rectangular channel waveguide with different length L using the TM_{10} mode. a) the transmission for different wavelengths, and b) the transmission peak for different channel length.

In order to further demonstrate the high sensitivity of this waveguide structure, the transmission characteristics of the proposed TM_{10} mode is utilized for enhanced transmission through a rectangular waveguide channel. The 3D FDTD provided by Lumerical has been employed for this purpose [19]. The input and output waveguides have cross sectional dimensions of $1.3 \times 1.9 \mu\text{m}$ and length of 700 nm each. The channel single mode waveguide is directly connected to the input and output waveguide. This channel waveguide has a cross sectional dimension of $650 \times 900 \text{ nm}$ which has a cutoff of the TM_{10} around 1600 nm . The length of the channel waveguide L is $1 \mu\text{m}$. Silver is utilized as the real metal for all the walls of the waveguides. The normalized transmission at the output waveguide is calculated and shown in Fig. 5. This normalized transmission is defined as the ration of the output transmitted power to the total input power. The transmission characteristics with higher refractive index are also calculated and demonstrated. It is clear that increasing the refractive index inside the channel waveguide should change the modal characteristics and shift the cutoff condition.

Thus, significant change in the transmission response is obtained particularly at wavelengths beyond the cutoff wavelength of the air filled channel. As an advantage of operation close to the cutoff wavelength, the transmitted field has minimum losses. The transmission and reflection characteristics for different channel lengths are given in Fig. 6. As shown in this figure, the increase in the insertion loss with the channel length is small. This insertion loss may include the reflected power and the propagation loss. It is clear that the reflected power is the dominant loss mechanism for such waveguides. Both the reflection and propagation loss are minimum close to the cutoff wavelength. Thus, working close to the cutoff wavelength allows for longer spatial interaction with the sensing material than what is available at any other wavelength band for the same insertion loss.

4. Rectangular waveguide for slow and fast light and negative index applications

The dispersion characteristics of SPPs waveguides can be engineered for applications such as slow light, fast light (negative group velocity) and negative index media (NIM). Exploiting the plasmonic waveguides for slow light application has been recently demonstrated using metal-insulator-metal (MIM) and insulator-metal-insulator (IMI) waveguide configurations [21]. Negative group velocity application has been also demonstrated. These configurations can also exhibit negative effective index of refraction. The effect has been theoretically and experimentally demonstrated [8–11]. The operating wavelength band and the bandwidth of this application are limited mainly by the type of the metal and filling dielectric material. Using MIM and IMI configurations limits the aforementioned applications to only one polarization. The rectangular waveguide is not only capable of obtaining the same functionality mentioned above, but also can relax the polarization restrictions for all these application. It can enable polarization insensitive version of these applications. For example, operating at the left edge of Region 1, high effective index can be obtained for slow light applications. More interestingly, being close to the peak of the curve also produces low dispersion or dispersion free regime, which is useful in producing highly compact delay lines for ultrafast bit rate data bus on chip.

It is well known that MIM structures exhibit negative dispersion for slot width of less than ~50 nm [8–11]. This negative dispersion (group velocity) is considered by the metamaterial community as a sufficient reason to obtain negative index media as the phase and the group velocities have opposite signs [8–11,22]. This negative index media was later experimentally demonstrated using the MIM configuration [8] and the FDTD simulation of a similar configuration has been also demonstrated [23]. However a theoretical analysis of the negative dispersion region of the MIM structure has recently been studied [24]. In this analysis, the causality is exploited to differentiate between the different sub-regions inside the negative dispersion regime. Defining these distinctions is mainly based on the sign of the imaginary part of the effective index, k , which in turn determines the direction of the traveling wave and decide if it is backward (negative index) or forward wave. According to this concept, the negative dispersion region is divided to three sub-regions. The first one is fast light with positive index and the second one is fast light with negative index. It is called fast light in this case mainly due to the fact that the peak of a light emerging from the negative group velocity media arrives before the peak of the input source [25]. The third sub-region is the negative index region, which occupies most of the bandwidth of the negative dispersion regime for the rectangular waveguide. According to the analysis given in [24], the negative refraction region is limited to the region that has positive values for the imaginary part of the effective refractive index k (backward wave region).

For rectangular metallic waveguides, if the same arguments discussed above are exploited, these sub-regions also appear in the rectangular waveguide for both the y -polarized and x -polarized, in Region 2 of the dispersion curve. However, the bandwidth of the first two sub-regions is limited to only few nanometers. In general, the backward wave sub-region occupies most of Region 2 and accordingly negative refraction is the dominant effect. For the rest of this work the backward wave region is defined as the region with positive k values not as the region of negative refraction to avoid confusion. We also provide some details about the backward wave region in rectangular waveguides and how it is affected by changing the design parameters.

As the rectangular waveguide has more degrees of freedom in the geometry than the MIM and IMI configuration, it can also allow for better bandwidth control. In this section, the effect of the design parameters on the performance and the dispersion characteristics of this waveguide is demonstrated. These design parameters include the material and the geometrical parameters of the metal and the dielectric media. The following analysis is limited only to the fundamental y -polarized mode only. This is mainly due to the blue shift of the spectrum of the x -polarized mode as shown in Fig. 2. The ability to exploit this mode for slow light or

negative refraction is limited to wavelength region close the UV regime which of interest to fewer applications hence will not be analyzed here.

4.1. Operating wavelength band

The propagation constant of the SPP mode at single interface is given by

$$k_{spp} = \frac{\omega}{c} \sqrt{\frac{\epsilon_d \epsilon_m}{\epsilon_d + \epsilon_m}} \quad (1)$$

As shown in Eq. (1), the propagation constant can be significantly increased in the range at which the real part of ϵ_d and ϵ_m are very close to each other. This region occurs when the frequency approaches $\omega^{spp} \approx \omega_p / \sqrt{1 + \epsilon_d}$.

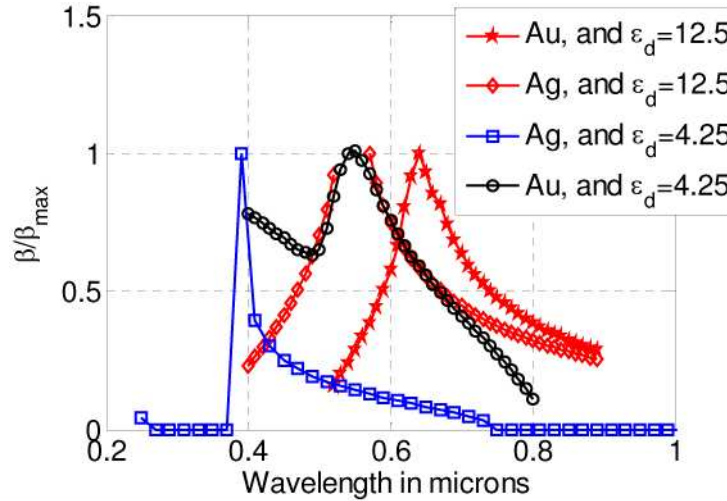


Fig. 7. The normalized dispersion characteristics of rectangular waveguide with 80x50 nm

Slow light applications can be obtained in this regime. The effective index and hence the propagation constant can reach high values if the operating wavelength is close to the resonance wavelength of the structure λ^{spp} as shown in Fig. 1. Phase delay and slow light applications can be exploited in this region accordingly.

For frequencies higher than ω^{spp} the group velocity is negative and the fundamental mode exhibits negative effective refractive index. The range at which the negative index of refraction occurs is given by

$$\lambda^p < \lambda < \lambda^{spp} \quad (2)$$

where

$$\lambda^{spp} \approx \lambda^p \sqrt{1 + \epsilon_d} \quad (3)$$

If the operating wavelength is in the proximity of λ^{spp} and lies in the region given in Eq. (2), then small values of the group velocity can also be obtained. This range can be utilized to obtain true delay-based application, where the phase and the group delay can be controlled through manipulating the waveguide parameters.

It is clear that the operating bandwidth is mainly determined by the plasma frequency of the metal ω_p and the dielectric constant of the core material through ω^{spp} . This dependence poses a fundamental limitation on the range of negative group velocity and slow light band. Using silver and high dielectric constant material of 12.5, this range can be obtained between

350 nm to 550 nm depending on the dimensions of the rectangular waveguide as shown in Fig. 7. However, this range can be red shifted if gold is utilized instead. This is mainly due to the lower plasma frequency of the gold. If using gold, the operating band can be shifted to be between 470 nm and 660 nm depending on the geometry. This wavelength can be further red shifted by using other Noble metals that have lower plasma frequencies such as copper.

Waveguides filled with Si_3N_4 have more relaxed constraints on the dimensions of the structure at which the negative refraction effects are obtained. The main drawback is the wavelength range at which this effect is obtained. For example, if the silver metal is utilized then this wavelength range is around the 400 nm. However, for gold metal this wavelength is shifted to be around 550 nm as can be seen in Fig. 7, where it imposes higher absorption.

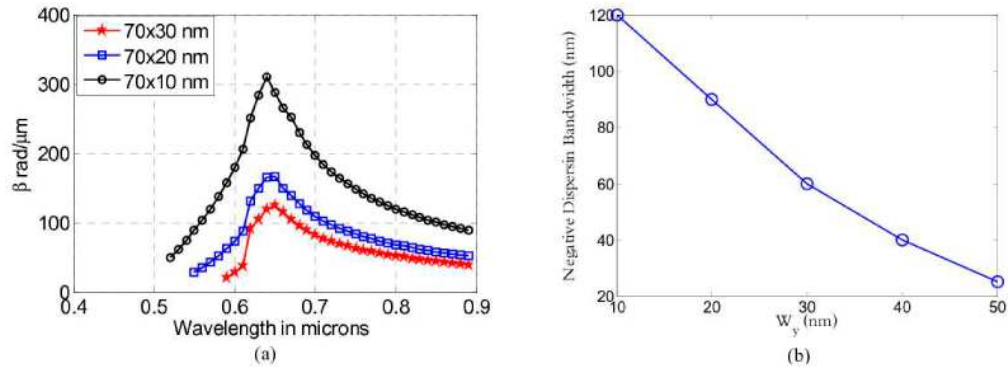


Fig. 8. a) The dispersion characteristics of gold metallic waveguide filled with $n_d = 3.5$ with for different waveguide heights. b) The change of the bandwidth of negative dispersion with the change of the heights for the same width of 70 nm.

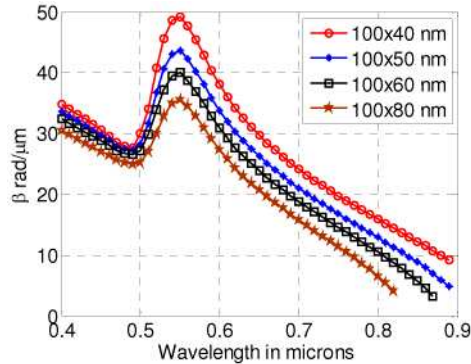


Fig. 9. The dispersion characteristics of gold metallic waveguide filled with Si_3Ni_4 with for different waveguide heights.

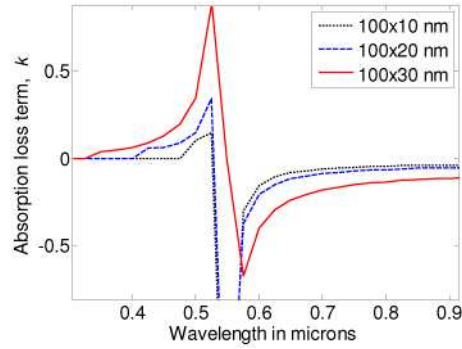


Fig. 10. The spectrum of the imaginary part of the effective index, k which defines the backward wave region in a rectangular waveguide with width of 100 nm and silver walls and filled with $n = 3.5$.

4.2 Bandwidth engineering

The bandwidth can be controlled through tuning the waveguide dimensions. These rectangular structures can provide wide bandwidth of operation specially for high index cores. It is clear from Fig. 8 that the bandwidth of the negative refraction region is increasing with the increase of the width of the metallic waveguide. The maximum attainable effective index also follows the same trend. The high index core filling enhances the dependence of the bandwidth of negative dispersion on the waveguide dimensions as shown in Figs. 8 and 9. The bandwidth of the negative dispersion also decreases with increasing the height and increases with the increase of the width of the waveguide. The same trend takes place for the backward wave region, as shown in Fig. 10.

4.3 Effect of design parameters on the propagation constant

The study of the effect of the design parameters on the value of the effective index is crucial to harness these effects. The possibility of obtaining high effective index is essential for slow light applications. The effect of the waveguide dimensions on the effective index value is studied and the results are shown in Figs. 11 and 12. It is clear from these figures that the effective index increases with the increase of the width and the reduction of the height of the

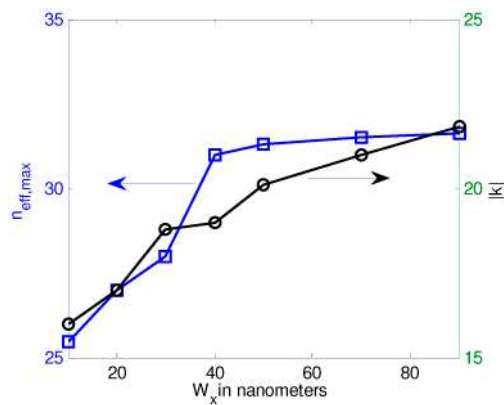


Fig. 11. , The maximum effective index of rectangular waveguide with gold metal and filled with $n_d = 3.5$ for fixed height, W_y , of 10 nm.

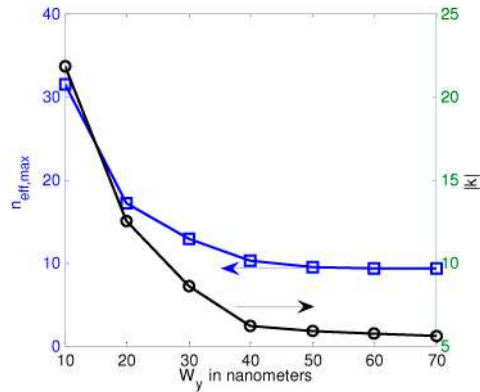


Fig. 12. The maximum effective index of rectangular waveguide with gold metal and filled with $n_d = 3.5$ for fixed width of 70 nm at wavelength of 633 nm.

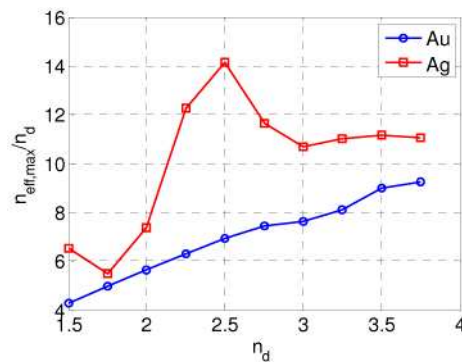


Fig. 13. The normalized values of the maximum effective index for different filled material for rectangular waveguide with 10x70 nm.

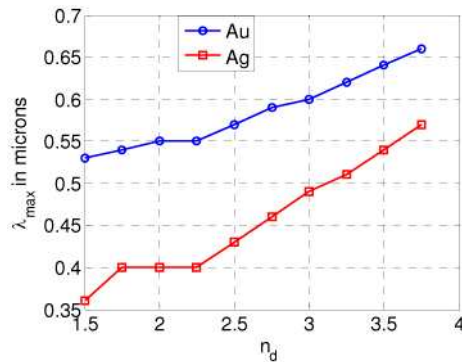


Fig. 14. The wavelengths at which the maximum values of the effective index occur for different filled material for rectangular waveguide with 10x70 nm.

waveguide. The imaginary part of the effective index, k represents the losses of this waveguide. It is clear from Figs. 11 and 12 that the real and the imaginary parts have a similar response to the changes in waveguide dimensions. It is also clear that the modal figure of merit $FOM = n_{eff}/k > 1$ for the entire operating range, which is a desirable feature for efficient, low insertion loss devices.

The effect of the core filling is also studied for different metal types. The normalized maximum effective indices and the wavelengths at which these values are obtained are given

in Figs. 13 and 14, respectively. The results are calculated for both gold and silver waveguides. The figures show that obtaining effective index of 35 is possible at different refractive index values of the core material, especially for silver. The wavelength at which these values are obtainable is at the edge of the visible band. Using gold metal values as high as 31.5 can be obtained in the middle of the visible wavelength range for a core material with a dielectric constant of 3.5.

4.4 Polarization insensitive designs

The polarization effect can be minimized if a square shape waveguide is utilized. This feature is also unique for the rectangular waveguide and unattainable for the MIM. The dimension of the square waveguide should be optimized to increase the bandwidth of the region where negative group velocity is obtained. From the calculations, it was found that increasing the waveguide dimensions reduces the bandwidth of operation of this device. For dielectric constant of 12.5 such as GaP or Silicon, the dimensions are limited to 30~50 nm. However, for Si₃N₄ the dimension can range from 50 nm up to few hundreds of nanometers depending on the metal type. The bandwidth of such structure is limited to 40~50 nm.

Square shape waveguides with gold boundaries, which are filled with high dielectric material core such as silicon, should be able to obtain negative index of refraction over a domain of 30~50 nm as discussed earlier. For example, a 25 × 25 nm waveguide with silicon filled can produce a negative index of refraction over a band from 600nm to 650nm. This proposed design of negative refraction metamaterial is insensitive to the polarization of the electric field in the plane of the surface.

5. Conclusion

The different key guided modes of the rectangular waveguide and their operating band are discussed. The application of this waveguide in sensing and energy transmission is examined and the potential application of the TM₁₀ for this purpose is also illustrated. The resemblances and difference between this waveguide and the MIM are also highlighted. The high sensitivity of these waveguides to the core material filling is also demonstrated and was shown to be higher than their counterparts and can reach four times the sensitivity obtained by MIM structures. High effective index for slow light applications are demonstrated. The effect of the design parameters on the maximum effective is also examined. Fast light operation region is defined and discussed. The possibility of obtaining polarization insensitive negative effective index media using this structure is also illustrated.